Carbohydrate Polymers 101 (2014) 289–300

Contents lists available at ScienceDirect

Carbohydrate Polymers

journal homepage: www.elsevier.com/locate/carbpol

Structural and functional properties of C-type starches

Jinwen Cai [a], Canhui Cai [a], Jianmin Man [a], Weidong Zhou [b], Cunxu Wei [a,*]

[a] Key Laboratories of Crop Genetics and Physiology of the Jiangsu Province and Plant Functional Genomics of the Ministry of Education, Yangzhou University, Yangzhou 225009, China
[b] Testing Center, Yangzhou University, Yangzhou 225009, China

ARTICLE INFO

Article history:
Received 18 May 2013
Received in revised form 12 August 2013
Accepted 16 September 2013
Available online 25 September 2013

Keywords:
C-type starch
Pea seed
Faba bean seed
Yam rhizome
Water chestnut corm
Structural and functional property

ABSTRACT

This study investigated the structural and functional properties of C-type starches from pea seeds, faba bean seeds, yam rhizomes and water chestnut corms. These starches were mostly oval in shape with significantly different sizes and contents of amylose, damaged starch and phosphorus. Pea, faba bean and water chestnut starches had central hila, and yam starch had eccentric hilum. Water chestnut and yam starches had higher amylopectin short and long chain, respectively. Water chestnut and faba bean starches showed C_A-type crystallinities, and pea and yam starches had C-type crystallinities. Water chestnut starch had the highest swelling power, granule swelling and pasting viscosity, lowest gelatinization temperatures and enthalpy. Faba bean starch had the lowest pasting viscosity, whereas yam starch had the highest gelatinization temperatures. Water chestnut and yam starches possessed significantly higher and lower susceptibility to acid and enzyme hydrolysis, the highest and lowest RDS contents, and the lowest and highest RS contents, respectively.

1. Introduction

Starch is stored as discrete semicrystalline granules in higher plants. There are three types of starches known as A-, B- and C-type according to their XRD (X-ray powder diffraction) patterns (Cheetham & Tao, 1998). The weight-average chain-lengths of the amylopectins of the A-, B-, and C-type starches are in the ranges 23–29, 30–44, and 26–29, respectively (Hizukuri, 1985). A- and B-type starches contain A- and B-type crystallinities, respectively. C-type starch is a mixture, and contains A- and B-type allomorphs within the same granule (Bogracheva, Morris, Ring, & Hedley, 1998; Buléon, Gérard, Riekel, Vuong, & Chanzy, 1998; Wang, Yu, Zhu, Yu, & Jin, 2009). Many researchers have reported the structural and functional properties of A- and B-type starches, however, there is little information on the properties of C-type starches.

Pea (*Pisum sativum*) seed is important for either human or livestock food. Starch is the most abundant carbohydrate in pea seed, and is used as an ingredient to modify the texture of food products (Simsek, Tulbek, Yao, & Schatz, 2009). Faba bean (*Vicia faba*) seed is a valuable source of energy due to its starch content, and is widely used for feed and food (Crépon et al., 2010). Yam (*Dioscorea opposita*) rhizome has been used as an important invigorant in traditional Chinese medicine for many years, is one of the most important substance with food and pharmaceutical functions. Starch is the major storage polysaccharides in yam rhizome (Wang et al., 2006). Water chestnut (*Eleocharis dulcis*) corm is rich in carbohydrates, especially starch, and is also a good source of dietary fiber, riboflavin, vitamin B_6, potassium, copper and manganese. The edible corm has long been valued throughout the Orient as a vegetable delicacy and as a source of medicine and starch (Hodge, 1956; Morton, 1988; Wang, Yin, Zhang, Xie, & Sun, 2008).

Previous reports show that starches from pea seeds, faba bean seeds, yam rhizomes and water chestnut corms are C-type starches (Ambigaipalan et al., 2011; Bogracheva et al., 1998; Cai & Wei, 2013; Wang et al., 2006). In this study, native starches were isolated from pea seeds, faba bean seeds, yam rhizomes and water chestnut corms. Their morphologies, sizes, amylose contents, damaged starch contents, phosphorus contents, molecular weight distributions, crystalline structures, thermal properties, swelling powers, granule swellings, pasting properties, hydrolysis properties, and digestion properties were investigated. The aim of this study was to compare the structural and functional properties of C-type starches

Abbreviations: AAG, *Aspergillus niger* amyloglucosidase; ATR-FTIR, attenuated total reflectance-Fourier transform infrared; ^{13}C CP/MAS NMR, solid-state ^{13}C cross-polarization magic-angle spinning nuclear magnetic resonance; DSC, differential scanning calorimetry; GPC, gel permeation chromatography; PPA, porcine pancreatic α-amylase; RDS, rapidly digestible starch; RS, resistant starch; RVA, rapid visco analyzer; SDS, slowly digestible starch; SEM, scanning electron microscope; XRD, X-ray powder diffraction.

* Corresponding author at: College of Bioscience and Biotechnology, Yangzhou University, Yangzhou 225009, China. Tel.: +86 514 87997217.
E-mail addresses: cxwei@yzu.edu.cn, yzuwcx@163.com (C. Wei).

0144-8617/$ – see front matter © 2013 Elsevier Ltd. All rights reserved.
http://dx.doi.org/10.1016/j.carbpol.2013.09.058

and determine their potential applications in food and nonfood industries.

2. Materials and methods

2.1. Plant materials

The seeds of pea (*P. sativum* L.) and faba bean (*V. faba* L.), the rhizomes of yam (*D. opposita* Thunb.) and the corms of water chestnut (*E. dulcis* (Burm. F.) Trin. Ex Hensch.) were used to isolate native starches. The mature dry seeds of pea and faba bean, and freshly harvested yam rhizomes and water chestnut corms were obtained from a local natural food market (Yangzhou City, China).

2.2. Isolation of native starch

Native starch granules were isolated following the method described by Cai and Wei (2013).

2.3. Morphology observation of starch

The starch granule micromorphology and "Maltese cross" were viewed with an Olympus BX53 polarized light microscope according to the method described by Cai and Wei (2013). For scanning electron microscope (SEM) observation, starch granules were suspended in anhydrous ethanol. One drop of the starch–ethanol suspension was applied to an aluminum stub using double-sided adhesive tape, and the starch was coated with gold using a sputter coater. Starch samples were observed and photographed using an environmental SEM (ESEM XL-30, Philips, Holland).

2.4. Particle size analysis of starch

Starch granules were stained in iodine solution (0.1% I_2, 1% KI) for 10 min in darkness. 10 μl of iodine-stained starch suspension was placed on the microscope slide and covered with a coverslip. The starch granules were viewed and photographed under the Olympus BX 53 light microscope equipped with a CCD camera. Images of starch granules were analyzed using JEDA-801D morphological image analysis system (Jiangsu JEDA Science-Technology Development Co., Ltd, Nanjing, China), which could give some information on long axis length, short axis length, long/short axis, area and circumference of granule. More than 2000 starch granules were analyzed per sample and grouped according to the long axis length. The number of starch granules in each group was counted.

2.5. Amylose content determination of starch

Amylose contents of starches were determined following a modified method (Man et al., 2012) according to the iodine colorimetry method of Konik-Rose et al. (2007). Apparent amylose content was evaluated from the absorbance of the starch–iodine mixture at 620 nm. The recorded value was converted to percent of amylose by reference to a standard curve prepared with amylose from potato (Sigma–Aldrich A0512) and amylopectin from corn (Sigma–Aldrich 10120).

2.6. Determination of damaged starch content

Damaged starch contents were determined by using Megazyme starch damage kit (based on AACC Method 76-31, Megazyme, K-SDAM). Briefly, 100 mg of starch was weighed out into centrifuge tubes. 1 ml of pre-equilibrated (at 40 °C for 5 min) fungal α-amylase solution (50 U/ml) was added. The tube contents were stirred for 5 s and incubated at 40 °C for exactly 10 min. 8 ml of 0.2% (v/v) sulphuric acid was then added and the tubes centrifuged at 1000 × *g* for 5 min. 0.1 ml of the supernatant was transferred to the bottom of a new test and treated with 0.1 ml of amyloglucosidase solution (2 U), and incubated at 40 °C for 10 min. 4 ml of glucose oxidase peroxidase solution was added to each tube, the mixtures incubated for 20 min at 40 °C and the absorbance read at 510 nm against a reagent blank.

2.7. Phosphorus content determination of starch

Phosphorus contents of starches were determined using the method of Noda et al. (2004) with some modifications. Briefly, 200 mg of starch was weighed out into a flask and heated with 4 ml of the mixture of conc. nitric acid and perchloric acid (4:1, v/v). When white smoke arose, the solution was cooled. Then, the volume was made up to 10 ml with distilled water. The phosphorus content in the digestion was measured as inorganic phosphorus, using the vanado-molybdate method to calculate the phosphorus content of starch. For assay, 5 ml of the solution of starch digestion, 3 ml of distilled water and 2 ml of coloring reagent (10 mM ammonium vanado, 20 mM ammonium molybdate, 25% conc. nitric acid) were mixed, kept for 15 min and the absorbance read at 400 nm.

2.8. GPC analysis of starch

Isolated native starches were deproteinizated and debranched with a modified method according to the methods of Borén et al. (2008) and Song and Jane (2000). Briefly, starch was washed five times with SDS-wash buffer (62.5 mM Tris–HCl, pH 6.8; 10 mM DDT; 10 mM EDTA, 4% SDS) to remove granule surface proteins, and then three times with water and two times with anhydrous ethanol. Starch was dried at 40 °C and passed through a 100-mesh sieve. Starch (50 mg) was moistened with 0.25 ml of water, and 4.75 ml of DMSO was added. The starch dispersion was heated in a boiling-water bath with stirring for 2 h and then stirred at 40 °C for 24 h. After centrifugation, the supernatant was precipitated (add 4 times of ethanol) for 2 h and centrifuged. The starch was dissolved in sodium acetate buffer (100 mM, pH 4.5) by heating and stirring in a boiling water bath for 1 h. The solution was cooled to room temperature, and isoamylase (250 U/mg starch) were added. The mixture was incubated for 36 h with stirring at 40 °C. The sample solution was then heated in a boiling water bath for 15 min to inactivate the enzyme. The sample slurries were frozen at −70 °C, and then freeze-dried. The molecular weight distributions of debranched starches were analyzed using gel permeation chromatography (GPC) according to the method of Cai and Shi (2010) with some modifications. The starch sample (5 mg) was mixed with DMSO (5 ml) and stirred in a boiling water bath for 2 h and then stirred at 40 °C for 24 h. The sample was filtered through a 2 μm filter and injected by an autosampler into a PL-GPC 220 high temperature chromatograph (Agilent Technologies UK Limited, Shropshire, UK) with three columns (PL110-6100, 6300, 6525) and a differential refractive index detector. The eluent system was DMSO containing 0.5 mM $NaNO_3$ at a flow rate of 0.8 ml/min. The column oven temperature was controlled at 80 °C. Standard dextrans with different molecular weight were used for molecular weight calibration.

2.9. XRD analysis of starch

XRD patterns of native and acid-modified starches were obtained on an XRD (D8, Bruker, Germany) following the method described by Wei, Xu, et al. (2010). For acid-modified starches, native starches were hydrolyzed in 2.2 M HCl at 35 °C for 10 days according to the method of Wei, Xu, et al. (2010).

2.10. Solid-state ^{13}C CP/MAS NMR analysis of starch

High-resolution solid-state ^{13}C cross-polarization magic-angle spinning nuclear magnetic resonance (^{13}C CP/MAS NMR) analysis of starch was carried out at $B_0 = 9.4$ T on a Bruker AVANCE III 400 WB spectrometer as described previously by Wei, Xu, et al. (2010). Before measurements, starch samples were stored in a desiccator, where a saturated solution of NaCl maintained a constant humidity atmosphere (relative humidity = 75%) for 1 week.

2.11. ATR-FTIR analysis of starch

Attenuated total reflectance-Fourier transform infrared (ATR-FTIR) spectra of starches were obtained on a Varian 7 000 FTIR spectrometer with a DTGS detector equipped with an ATR single reflectance cell containing a germanium crystal (45° incidence-angle) (PIKE Technologies, USA) as previously described by Wei, Xu, et al. (2010). Original spectra were corrected by a baseline in the region from 1200 to 800 cm^{-1} before deconvolution was applied using Resolutions Pro. The assumed line shape was Lorentzian with a half-width of 19 cm^{-1} and a resolution enhancement factor of 1.9.

2.12. Thermal property of starch

Thermal properties of starches were measured using a differential scanning calorimetry (DSC) (200-F3, NETZSCH, Germany) as described previously by Wei et al. (2011).

2.13. Swelling power determination of starch

Swelling powers of starches were determined by heating starch–water slurries in a water bath at temperatures ranging from 40 to 95 °C at 5 °C intervals according to the method of Wei et al. (2011).

2.14. Granule swelling determination of starch

Starch suspensions were prepared by suspending about 10 mg starch in 1.0 ml of distilled water by using a vortex mixer. The suspension was transferred onto a slide, covered with a coverslip, and sealed with nail polish to prevent moisture loss during heating. The sealed specimen was then mounted on a Kitazato hot stage apparatus and observed under a long focus M Plan Semi Apochromat objective using an Olympus microscope. The hot stage was heated from 25 to 40 °C at a heating rate of 5 °C/min and from 40 to 95 °C at a heating rate of 1 °C/min. The swelling of individual starch granule during heating was viewed and photographed using an Olympus DP72 CCD camera from 40 to 95 °C at 5 °C intervals. The area of starch granule was analyzed from the micrograph with JEDA 801D morphological image analysis system (Jiangsu JEDA Science-Technology Development Co., Ltd, Nanjing, China). Over 50 starch granules were measured per sample. The granule swelling was presented as area swelling ratio (ASR) from ungelatinized granule at 40 °C, and calculated by the equation: ASR = At/Ai, where Ai and At represented the area of starch granule at initial (40 °C) and specific testing temperature, respectively.

2.15. Pasting property of starch

Pasting properties of starches (8% solids) were evaluated with a Rapid Visco Analyzer (RVA) (RVA-3D, Newport Scientific, Narrabeen, Australia). A Programmed heating and cooling cycle was used, where the samples were held at 50 °C for 1 min, heated to 95 °C at a rate of 12 °C/min, maintained at 95 °C for 2.5 min, cooled to 50 °C at a rate of 12 °C/min, and then held at 50 °C for 1.4 min. Parameters recorded were pasting temperature, peak viscosity, hot viscosity, final viscosity, breakdown viscosity (peak-hot viscosity) and setback viscosity (final-hot viscosity).

2.16. Hydrolysis rate of starch

Starches were hydrolyzed by porcine pancreatic α-amylase (PPA) (Sigma–Aldrich A-3176), *Aspergillus niger* amyloglucosidase (AAG) (Sigma–Aldrich A-7095) and HCl. The hydrolysis process was performed following a modified method (Man et al., 2012) according to the method of Li, Vasanthan, Hoover, and Rossnagel (2004). After hydrolysis, starch slurries were quickly centrifuged (5000 × *g*) at 4 °C for 10 min. The supernatant was used for measurement of the solubilized carbohydrates to quantify the degree of hydrolysis by the anthrone–H_2SO_4 method (Viles & Silverman, 1949).

2.17. In vitro digestion analysis of starch

In vitro starch digestion was analyzed following a modified method (Carciofi et al., 2012) according to Englyst procedure (Englyst, Kingman, & Cummings, 1992), using native raw starch, gelatinized starch (98 °C, 12 min), and retrograded starch i.e. gelatinized starch re-crystallized for 36 h at 4 °C. 10 mg of starch was incubated in 2 ml of enzyme solution (20 mM sodium phosphate buffer, pH 6.0, 6.7 mM NaCl, 0.01% NaN_3, 2.5 mM $CaCl_2$, 4 U PPA (Sigma A3176), 4 U AAG (Megazyme E-AMGDF)) at 37 °C for 20 min and 1, 2, 6, 12 and 24 h. Enzyme treatment was terminated by adding 240 μl 0.1 M HCl and 2 ml of 50% ethanol on ice and centrifuged (14,000 × *g*, 5 min). The supernatant and starch residue were collected. The amounts of soluble carbohydrates and glucose were determined by the anthrone–H_2SO_4 and D-glucose (GOPOD Format) assay kit (Megazyme, K-GLUC), respectively. Starch nutritional fractions based on the rate of hydrolysis were rapidly digestible starch (RDS, digested within 20 min), slowly digestible starch (SDS, digested between 20 and 120 min) and resistant starch (RS, undigested after 120 min). The starch residue was washed three times with water and fixed with 2.5% glutaraldehyde at 4 °C for morphology observation.

2.18. Statistical analysis

The data reported in all the tables were mean values and standard deviations. Analysis of variance (ANOVA) by Tukey's test ($P < 0.05$) was evaluated using the SPSS 16.0 Statistical Software Program.

3. Results and discussion

3.1. Morphology and size distribution of starch

Light micrographs of starches taken under normal light and polarized light are presented in Fig. 1. Most of water chestnut starch granules were oval or spherical, even though some polyhedral granules were also observed. All the water chestnut starch granules had the typical "Maltese crosses" with the hila in the center of granules. A small quantity of water chestnut starch had the damaged granules. Yam starch granules were oval shapes and exhibited strong birefringence patterns with the hila at one end of granules. Most of pea and faba bean starch granules were elliptical shapes with large sizes, and some were spherical shapes with small sizes. The spherical granules exhibited the typical "Maltese cross", showing a dark cross in the center, whereas the elliptical granules had a different birefringence pattern with two cross lines at the two ends of the granule and a dark line in the center. Some large granules also showed multiple "Maltese crosses" on birefringence. Similar observation on granule shapes and "Maltese crosses" of pea and faba bean starches has been reported by Chung and Liu (2012)

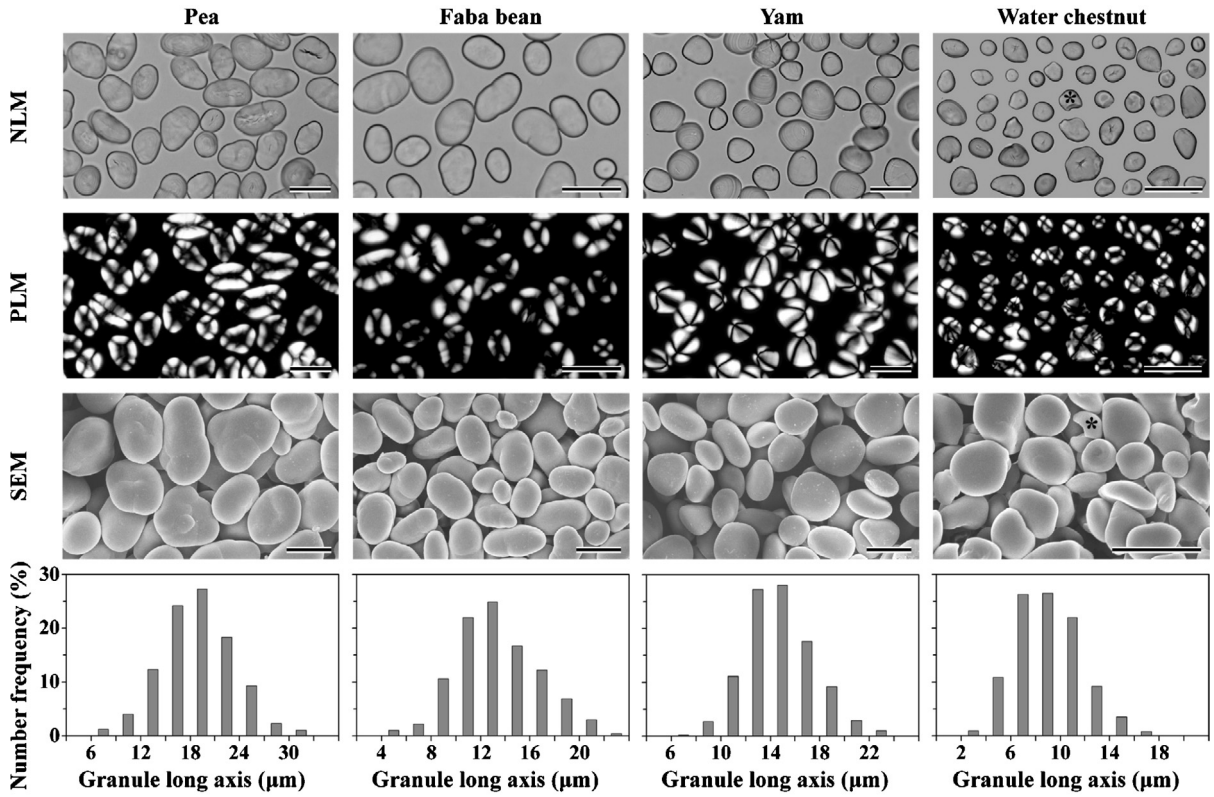

Fig. 1. Morphologies and size-distributions of starch granules. NLM, light micrographs under normal light; PLM, light micrographs under polarized light; SEM, scanning electron micrographs. Asterisk showed the damaged starch granule. Scale bar = 20 μm.

and Ambigaipalan et al. (2011). The birefringence patterns indicate that amylopectin crystallites are arranged radially within the granule at right angles to the surface with their single reducing end group toward the hilum (Ambigaipalan et al., 2011). The hilum is commonly situated near the middle of the granule, but it can be eccentric. The shape of hilum may be in the form of a point, stellate and radiating from the center, or elongated and branched in the interior of granule (Wei, Qin, et al., 2010). Starch granule, which has many hila in one granule, shows many birefringence patterns (Wei, Qin, et al., 2010). In this paper, pea and faba bean starches had different "Maltese cross" patterns, which might result from the different position, shape and quantity of hilum in the granule. The differences in granule shape and hilum position might be attributed to the biological origin, biochemistry of the amyloplast, and physiology of the plant (Sandhu, Singh, & Kaur, 2004).

SEM was used to further observe the submicroscopic shape and surface characteristic of starch granule (Fig. 1). The shapes of pea, faba bean, yam and water chestnut starches under SEM were similar to those under light microscope. The surface of these starch granules was all smooth and did not show any pores and fissures. Though pea, faba bean and water chestnut starch granules were all intact, some damaged granules were viewed in water chestnut starch, which was in agreement with the observation of light microscope.

Starch granule sizes are usually measured by electrozone, image analysis, or laser light-scattering analysis methods. Harrigan (1997) found that using image analysis to determine starch granule size could yield accurate and reproducible data. In this study, starch granule sizes were measured by image analysis, the plots of number percent of granules over a range of the long axis length were shown in Fig. 1. Pea, faba bean, yam and water chestnut starches all showed unimodal size distributions. The statistical analysis of particle size is shown in Table 1. The starches showed significantly different granule sizes, pea and water chestnut starches had the largest and lowest granule sizes, respectively.

3.2. Contents of amylose, damaged starch and phosphorus of starch

The amylose content plays an important role in starch internal quality. The apparent amylose contents of pea, faba bean, yam and water chestnut starches are presented in Table 1. Water chestnut and pea starches had the lowest (27.9%) and highest (44.4%) amylose contents, respectively. Granular integrity can be affected by the mechanical action of starch isolation process. Starch damage profoundly changes starch granule structure and it influences functional properties of starch. In this paper, the damaged starch content is determined and shown in Table 1. Water chestnut had more damaged starch (1.57%) than pea (0.16%), faba bean (0.19%) and yam (0.11%). The water chestnut starch granules had the smallest size and the isolation process of starch was basically the same among the four starches. Therefore, the higher content of damaged starch indicated that water chestnut starch granules were easily destroyed by mechanical isolation. As shown in Table 1, the phosphorus content ranged between 48.2 and 223.6 ppm among four starches. Faba bean and yam starches had the lowest and highest phosphorus content, respectively. The starches from different botanical sources have different phosphorus contents, and the growing environment, especially the temperature, affects the phosphorus content (Noda et al., 2004).

3.3. Molecular weight distribution of starch

The molecular weight distributions of isoamylase-debranched starches as determined by GPC are shown in Fig. 2. The GPC parameters are summarized in Table 2. A trimodal distribution of low,

Table 1
Granule sizes and contents of amylose, damaged starch and phosphorus of starches.

Starches	Size			Amylose content (%)	Damaged starch content (%)	Phosphorus content (ppm)
	Long axis length (μm)	Short axis length (μm)	Long/short axis			
Pea	19.0 ± 4.4d	13.4 ± 2.7d	1.42 ± 0.21c	44.4 ± 1.3d	0.16 ± 0.03ab	139.2 ± 5.7c
Faba bean	13.5 ± 3.4b	9.7 ± 2.1b	1.39 ± 0.23b	40.0 ± 0.5c	0.19 ± 0.03b	48.2 ± 2.8a
Yam	14.8 ± 2.8c	11.0 ± 2.6c	1.38 ± 0.29b	34.7 ± 0.9b	0.11 ± 0.02a	223.6 ± 6.6d
Water chestnut	9.1 ± 2.6a	7.2 ± 2.0a	1.28 ± 0.19a	27.9 ± 0.6a	1.57 ± 0.05c	93.9 ± 3.7b

Data were means ± standard deviations ($n > 2000$ for sizes and = 3 for contents of amylose, damaged starch and phosphorus). Values in the same column with different letters were significantly different ($p < 0.05$).

Table 2
GPC parameters of isoamylase-debranched starches.

Starches	Peak area (%)			Peak 1/Peak 2[a]	Degree of polymerization[b]	
	Peak 1	Peak 2	Peak 3		Peak 1	Peak 2
Pea	40.6 ± 0.2a	25.4 ± 0.3b	34.1 ± 0.5b	1.60 ± 0.01b	12.3 ± 0.7b	56.2 ± 1.0a
Faba bean	43.0 ± 0.4b	25.6 ± 1.2ab	31.5 ± 0.8b	1.69 ± 0.10b	12.5 ± 0.0b	51.9 ± 2.2a
Yam	40.4 ± 0.2a	33.4 ± 0.1c	26.3 ± 0.4a	1.21 ± 0.00a	12.7 ± 0.2b	60.1 ± 0.5b
Water chestnut	52.1 ± 1.0c	23.3 ± 0.4a	24.7 ± 0.6a	2.24 ± 0.08c	9.9 ± 0.1a	53.8 ± 0.5a

Data were means ± standard deviations ($n = 2$). Values in the same column with different letters were significantly different ($p < 0.05$).
[a] The data were determined according to the area ratio of Peak 1 and Peak 2.
[b] The degrees of polymerization were obtained from the maximum height of the peak.

middle and high molecular weight peaks, designated Peak 1, Peak 2 and Peak 3, respectively, was observed. Peak 1 and Peak 2 consist of short (A and short B chains) and long (long B chains) branch chains of amylopectin, respectively. Peak 3 includes amylose (Song & Jane, 2000). The present results suggested that water chestnut starch had a significantly higher proportion of amylopectin short chains. Yam starch had significantly higher amylopectin long chains, water chestnut and yam starches had similar amylose contents, which were significantly lower than that of pea and faba bean starches. Debranched starch consists of amylopectin short chain (DP 6-36), amylopectin long chain (DP 37–120), intermediate chain (DP 120–1000) and amylose chain (DP ≥1000) on the basis of the demarcations defined for molecular size distribution (Butardo et al., 2012). The intermediate chain contains both linear and branched components (Shi, Capitani, Trzasko, & Jeffcoat, 1998). The amylose content determined based on iodine and starch affinity is described as apparent amylose content, which overestimates amylose content if there are branched molecules with long side chains that bind iodine (Shi et al., 1998). The present results showed that apparent amylose content obtained by iodine colorimetry method (Table 1) was significantly higher than the amylose content determined by GPC (Table 2), which was in agreement with the report of Shi et al. (1998) and suggested that the intermediate chain and longer amylopectin branched chain could bind iodine to increase the value of apparent amylose content. The results of apparent amylose content (Table 1) and GPC (Fig. 2 and Table 2) all showed that water chestnut starch had significantly lower content of intermediate length chains than pea, faba bean and yam starches.

Peak 1 contains A and short B chains of amylopectin, and Peak 2 includes long B chains of amylopectin. The area ratio of Peak 1 to Peak 2 might be used as an index of the extent of branching of amylopectin; the higher the ratio, the higher the degree of branching (Wang, White, Pollak, & Jane, 1993). Water chestnut and yam starches had the highest and lowest branching degree of amylopectin among four starches, respectively (Table 2). The degrees of polymerization of Peak 1 and Peak 2 at the maximum height of the peak were also calculated and presented in Table 2. Water chestnut starch had the lowest polymerization degree of short chain of amylopectin, and yam starch had the highest polymerization degree of long chain of amylopectin.

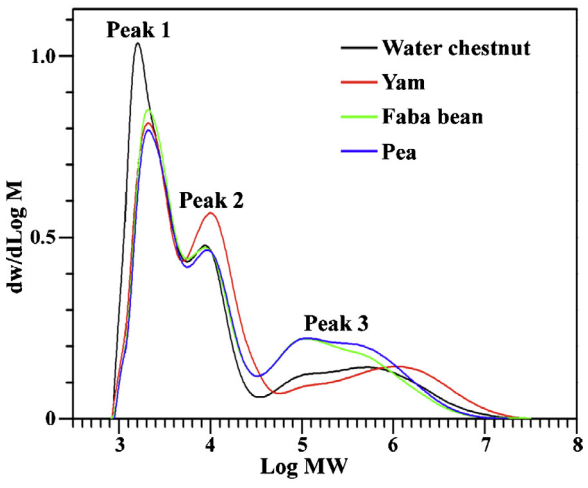

Fig. 2. GPC profiles of isoamylase-debranched starches.

3.4. XRD spectrum of starch

The XRD spectra of pea, faba bean, yam and water chestnut starches are shown in Fig. 3A. XRD pattern of A-type starch shows strong diffraction peaks at about 15° and 23° 2θ, and an unresolved doublet at around 17° and 18° 2θ. That of B-type starch has the strongest diffraction peak at around 17° 2θ, a few small peaks at around 15°, 20°, 22° and 24° 2θ, and a characteristic peak at about 5.6° 2θ. C-type starch is a mixture of both A- and B-type crystallinities, and can be further classified to C_A-type (closer to A-type), C-type and C_B-type (closer to B-type) according to the proportion of A- and B-type allomorphs. XRD pattern of typical C-type starch gives singlet peaks at about 17° and 23° 2θ, and a few small peaks at around 5.6° and 15° 2θ. The XRD patterns of C_A- and C_B-type starches are similar to that of C-type, but there is a shoulder peak at about 18° 2θ and a strong singlet peak at 23° 2θ for C_A-type starch, and two shoulder peaks at about 22° and 24° 2θ for C_B-type starch (Cai & Wei, 2013; Cheetham & Tao, 1998). According to XRD patterns (Fig. 3A), native pea and yam starches were C-type

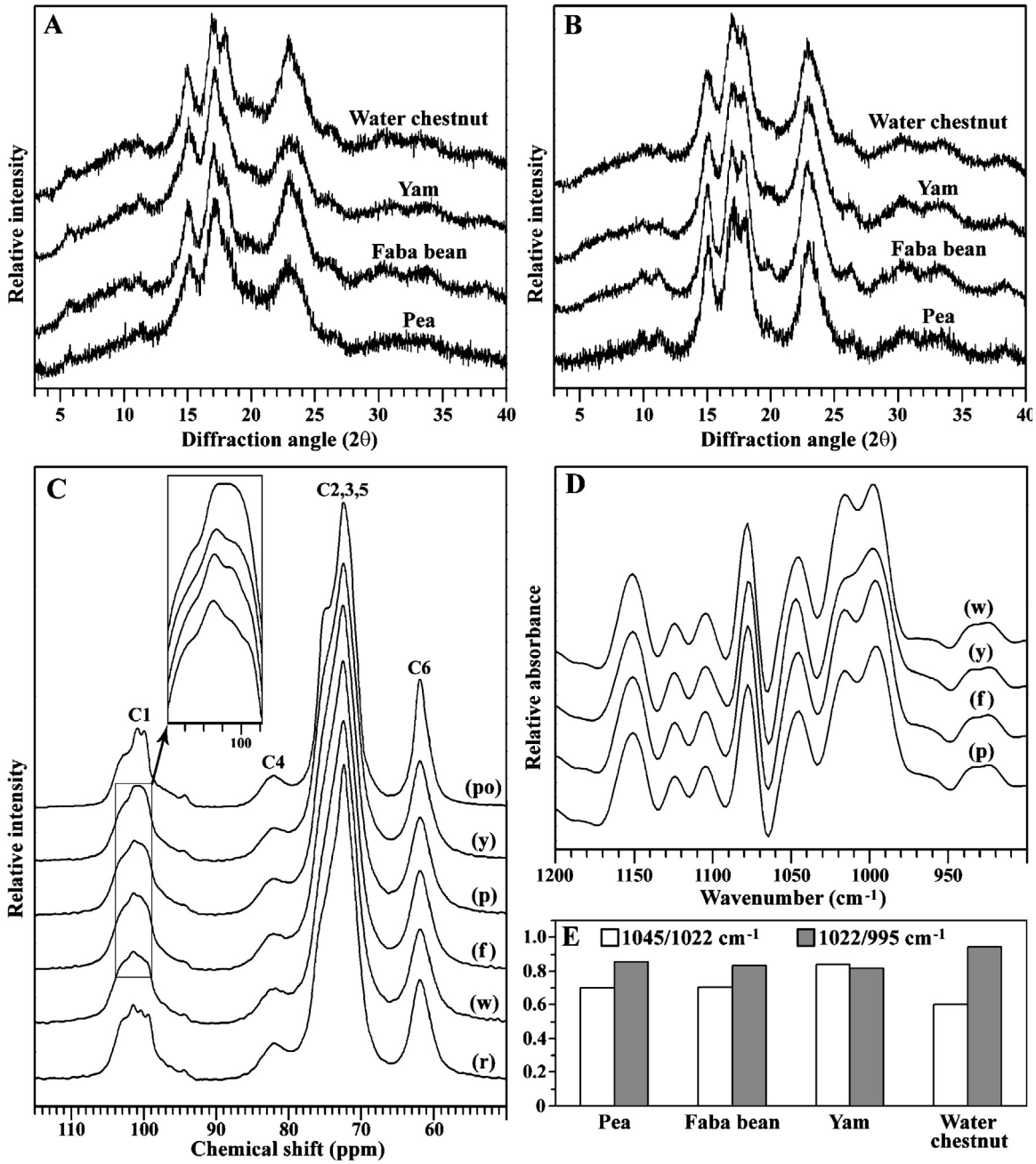

Fig. 3. Spectrum analyses of starches. (A) XRD spectra of starches; (B) XRD spectra of acid-modified starches by HCl for 10 days; (C) ^{13}C CP/MAS NMR spectra of starches; (D) deconvoluted ATR-FTIR spectra of starches; (E) IR ratio of starches. f, faba bean; p, pea; po, potato; r, rice; w, water chestnut; y, yam.

crystallinities, and faba bean and water chestnut starches were C_A-type crystallinities, which were in agreement with previous reports (Ambigaipalan et al., 2011; Bogracheva et al., 1998; Cai & Wei, 2013; Wang et al., 2006).

C-type starch consists of A- and B-type allomorphs within the granule. Acid modification does not change the crystalline characteristics of A- and B-type starches, and is commonly used to investigate the allomorph distribution of C-type starch (Wang et al., 2009). The XRD spectra of acid-modified pea, faba bean, yam and water chestnut starches all showed that the peak at 5.6° 2θ disappeared, the peak at 18° 2θ appeared, and the peak at 23° 2θ sharpened, which indicated that acid-modified starches gave A-type crystallinities (Fig. 3B). This result revealed that the B-type allomorph in the C- or C_A-type starches was first degraded or degraded faster than A-type allomorph during the process of acid hydrolysis. Generally, starch granule is hydrolyzed by HCl from interior to outer region (Wang et al., 2009). Therefore, the crystalline change of acid-modified starches indicated that the B-type allomorph existed in the interior of C-type starch granules, which was surrounded by the A-type allomorph at the periphery of starch granule. This crystalline granular structure of C-type starch was in agreement with that of previous reports (Bogracheva et al., 1998; Wang et al., 2009).

3.5. ^{13}C CP/MAS NMR spectrum of starch

The solid-state ^{13}C CP/MAS NMR patterns for starches are shown in Fig. 3C. The resonances at different ppm were assigned

Table 3
DSC parameters of starches.

Starches	T_o (°C)	T_p (°C)	T_c (°C)	ΔT (°C)	ΔH (J/g)
Pea	59.5 ± 0.4b	66.4 ± 0.1b	73.8 ± 0.2b	14.3 ± 0.3b	12.5 ± 0.3bc
Faba bean	65.6 ± 0.3c	71.3 ± 0.1c	78.2 ± 0.3c	12.6 ± 0.3a	12.2 ± 0.3b
Yam	69.6 ± 0.4d	76.8 ± 0.1d	89.9 ± 0.3d	20.3 ± 0.4d	13.1 ± 0.4c
Water chestnut	49.8 ± 0.2a	57.9 ± 0.1a	68.7 ± 0.3a	18.9 ± 0.3c	8.9 ± 0.3a

Data were means ± standard deviations ($n = 3$). Values in the same column with different letters were significantly different ($p < 0.05$). T_o, onset temperature; T_p, peak temperature; T_c, conclusion temperature; ΔT, gelatinization range ($T_c - T_o$); ΔH, enthalpy of gelatinization.

according to the literature reports (Bogracheva, Wang, & Hedley, 2001). The C1 resonance, which contains information on both the crystalline nature and the noncrystalline (but rigid) chains, has been employed to examine the structure of different type starches. The multiplicity of the C1 resonance corresponds to the packing type of the starch granule. The C1 peak of spectrum is a triplet for A-type starch, and a doublet for B-type starch (Atichokudomchai, Varavinit, & Chinachoti, 2004). In general, the C-type starch also shows triplet C1 spectrum if the A-type crystalline structure is predominant in the sample, and doublet C1 spectrum if the B-type crystalline structure is predominant (Bogracheva et al., 2001). In this paper, the ^{13}C CP/MAS NMR spectra of pea, faba bean, yam and water chestnut starches were compared with that of rice A-type starch and potato B-type starch (Fig. 3C). Rice starch occurred as typical triplets at about 99.5, 100.5 and 101.5 ppm, and potato starch doublets at about 100 and 101 ppm. Water chestnut and faba bean starches showed inconspicuous triplets, and pea and yam starches presented inconspicuous doublet. These results in combination with XRD patterns further showed that starches from water chestnut and faba bean starches were C_A-type crystallinity and pea and yam starches were C-type crystallinity.

3.6. ATR-FTIR spectra of starch

The development of sampling devices like ATR-FTIR combined with procedures for spectrum deconvolution provides opportunities for the study of starch external region structure (Sevenou, Hill, Farhat, & Mitchell, 2002). The deconvoluted ATR-FTIR spectra in the region 1200–900 cm^{-1} of starches from pea, faba bean, yam and water chestnut are presented in Fig. 3D. The bands at 1045 cm^{-1} are linked with order/crystalline regions in starch. The 1022 cm^{-1} absorbance band arises as a result of absorption by stretching modes in amorphous starch, and is therefore sensitive to amorphous structure. The band at 995 cm^{-1} results from bonding in hydrated carbohydrate helices. The ratio of absorbance 1045/1022 cm^{-1} is used to quantify the degree of order, and that of 1022/995 cm^{-1} can be used as a measure of the proportion of amorphous to ordered carbohydrate structure in the starch. The intensity ratios of 1045/1022 and 1022/995 cm^{-1} are therefore useful as a convenient index of FTIR data in comparisons with other measures of starch conformation (Sevenou et al., 2002; Warren, Royall, Gaisford, Butterworth, & Ellis, 2011). The ratios for 1045/1022 and 1022/995 cm^{-1} of starches are shown in Fig. 3E. Based on both the spectra and calculated data, starches showed significant difference in the ordered structure of starch external region. Yam and water chestnut starches had the highest and lowest ordered degree in granule external region, respectively (Fig. 3D and E) though FTIR is not able to differentiate starch crystal type. The native starches with the same crystal type always show similar ratio for 1022/995 cm^{-1}. The band at 1022 cm^{-1} of C-type starch is weaker than that of A-type starch and stronger than that of B-type starch (Sevenou et al., 2002). The spectrum and the IR ratio for 1022/995 cm^{-1} showed that pea, faba bean, yam and water chestnut starches were C-type crystallinities, which was in agreement with the XRD patterns.

3.7. Thermal properties

Thermal properties of pea, faba bean, yam and water chestnut starches were determined by using a DSC, and their thermal parameters are given in Table 3. Water chestnut starch had the lowest gelatinization temperatures and enthalpy, which suggested that less energy was required to initiate gelatinization. The highest values for gelatinization temperatures and enthalpy were recorded for yam starch. Pea and faba bean showed similar gelatinization properties. In this paper, the thermal properties of pea, faba bean and yam starches were similar to the reports of Chung and Liu (2012), Ambigaipalan et al. (2011), and Wang et al. (2006). However, the thermal parameters of water chestnut starch were significantly different with the reports of Xu and Shoemaker (1986) and Wang et al. (2008). Xu and Shoemaker (1986) found that the gelatinization temperatures of water chestnut starch were 59.0 °C for onset temperature, 70.4 °C for peak temperature, and 82.8 °C for conclusion temperature. Wang et al. (2008) reported that DSC parameters of water chestnut starch was 58.5 °C for onset temperature, 64.1 °C for peak temperature, 68.4 °C for conclusion temperature, and 10.8 J/g for gelatinization enthalpy. The peak and conclusion temperatures of water chestnut starch in the report of Wang et al. (2008) were significantly lower than that of Xu and Shoemaker (1986). In this paper, the conclusion temperature and enthalpy of water chestnut starch was similar to the results of Wang et al. (2008).

The thermal property of starch is related to a variety of factors including the size, granule ultrastructure, amylose content, amylopectin branch chain, phosphorus content, damaged starch content, and crystalline structure. The content of amylopectin short chain plays a more important role than the amylose content in accounting for DSC gelatinization properties. A larger amount of extremely short chains in amylopectin molecules reduces the efficiency of packing in the starch crystallinity, resulting in lower gelatinization temperature and enthalpy (Noda et al., 2004). It is known that physical damage converts the large ordered regions into disorderly amorphous materials, freely accessible to water. The damaged starches have lower gelatinization temperature and enthalpy than undamaged starches (Morrison, Tester, & Gidley, 1994). In this paper, water chestnut starch had the smallest granule size, lowest amylose content and structure ordered degree, and highest contents of amylopectin short chain and damaged starch among four starches (Tables 1 and 2, Fig. 3). These properties might be responsible of the lower gelatinization temperatures and enthalpy of water chestnut starch. The granule size, crystalline structure, and contents of amylose, amylopectin short chain and phosphorus of starch are influenced by different cultivars, cultivated condition and environment. Water chestnut has many cultivars in different regions in China. The gelatinization temperature of water chestnut starch was lower than the previous reports (Wang et al., 2008; Xu & Shoemaker, 1986), which might be due to different cultivars and growing regions.

3.8. Swelling power of starch

According to starch gelatinization temperatures (Table 3), the swelling powers of pea, faba bean, yam and water chestnut

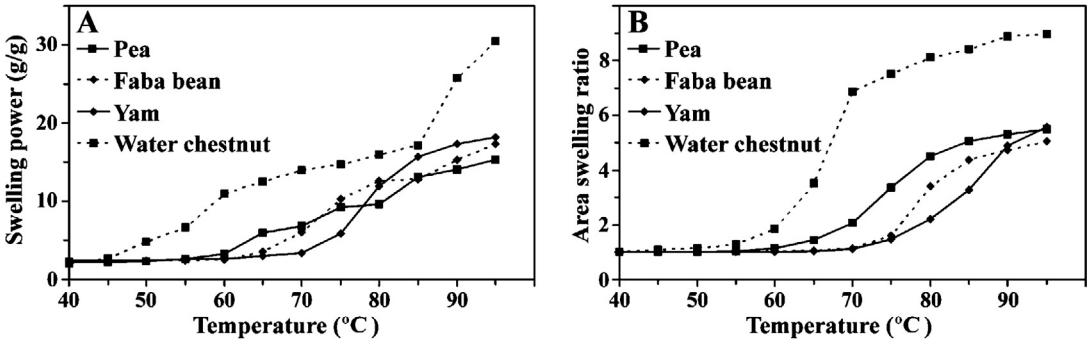

Fig. 4. Swelling powers (A) and area swelling ratios (B) of starch granules.

starches were investigated from 40 °C to 95 °C at 5 °C intervals (Fig. 4A). Before gelatinization, swelling powers slightly increased with increasing temperature. After gelatinization, swelling power quickly increased. A sharp increase in swelling power of water chestnut starch was observed from 50 °C, while that of yam starch from 75 °C. Water chestnut starch had a much higher swelling power during heating compared with that of the other starches. Swelling power can be used to assess the extent of interaction between the starch chains, within the amorphous and crystalline of the starch granule. The swelling power of starch has been reported to depend upon the water holding capacity of starch molecules by hydrogen bonding. Hydrogen bonds stabilizing the structure of the double helices in crystallites are broken during gelatinization and are replaced by hydrogen bonds with water (Tester & Karkalas, 1996). Damaged granules are easily hydrated and have higher swelling factors than the intact granules in cold water; however swelling of granules beyond gelatinization temperature is dependent on the level of damage and types of starches (Tester, 1997). Amylose restrains starch swelling and maintains the integrity of swollen granules (Sasaki & Matsuki, 1998). Water chestnut starch had higher damaged starch and lower amylose content and gelatinization temperature (Table 1, Table 3), which might result in that it had significantly higher swelling power than pea, faba bean and yam starches during heating (Fig. 4A).

3.9. Granule swelling of starch

The granule swelling of starch was in situ observed under light microscope with a hot stage and presented as area swelling ratio from ungelatinized granules at 40 °C. The area swelling ratios of pea, faba bean, yam and water chestnut starch granules at 5 °C intervals from 40 to 95 °C are shown in Fig. 4B. Different starches showed significantly different granule swelling processes. Water chestnut starch granules began to swell at 55 °C, pea starch at 65 °C, and faba bean and yam starch granules at 75 °C. The trend of starch granule swelling was similar to that of their swelling powers during heating. Water chestnut starch had the highest granule swelling among four starches during heating, which might result from its lower amylose content and gelatinization temperature.

3.10. Pasting property of starch

Pasting properties of starches measured by RVA are summarized in Table 4. The RVA parameters were significantly different among four C-type starches. Faba bean and water chestnut starches showed the lowest and highest pasting viscosities, respectively. The pasting temperature of water chestnut starch was the lowest (63.5 °C), whereas that of yam starch was the highest (83.1 °C).

The pasting properties of starches have been reported to be influenced by size, rigidity, amylose to amylopectin ratio and swelling power of the granules (Singh, Kaur, Ezekiel, & Guraya, 2005). The amylose content may be the major factor affecting the starch pasting properties, since the extent of starch swelling is assumed to be inhibited by an increase of amylose content. Therefore, starch with lower amylose content has been assumed to exhibit higher pasting viscosity and lower pasting temperature (Noda et al., 2004). Damaged starch granules can absorb water, swell and leach out amylose and amylopectin, which causes an increase in the viscosity of starch (Barrera et al., 2013). Pasting temperature corresponds to the swelling power of starch. High pasting temperature indicates high resistance to swelling (Wang et al., 2008). The higher pasting viscosity and lower pasting temperature of water chestnut starch might result from lower amylose content, higher granule swelling, higher swelling power, and higher damaged starch content.

3.11. Hydrolysis property of starch

The hydrolysis degrees of pea, faba bean, yam and water chestnut starches by HCl are presented in Fig. 5A. The hydrolysis degree increased gradually with increasing acid hydrolysis time. The differences among the hydrolysis degrees of four C-type starches after hydrolysis suggested that water chestnut and yam starches showed the lowest and highest resistant ability to acid, respectively.

The time courses of PPA and AAG hydrolysis of starches are presented in Fig. 5B and C. The hydrolysis was biphasic, a relatively rapid rate at the initial stage, followed by a progressively decreased rate thereafter. A biphasic trend of amylase hydrolysis has also been observed in starches (Li et al., 2004). Water chestnut and yam starches had the highest and lowest hydrolysis degrees of

Table 4
Pasting properties of starches.

Starches	V_P (mPa s)	V_H (mPa s)	V_B (mPa s)	V_F (mPa s)	V_S (mPa s)	P_{Temp} (°C)
Pea	3131.7 ± 60.9b	2375.3 ± 72.7b	756.3 ± 89.6b	4199.0 ± 92.1b	1823.7 ± 86.5a	77.9 ± 0.3c
Faba bean	2629.7 ± 12.4a	2082.0 ± 21.6a	547.7 ± 9.7a	3850.3 ± 42.0a	1768.3 ± 32.7a	75.8 ± 0.0b
Yam	4268.0 ± 77.8c	3421.7 ± 30.9c	846.3 ± 46.9b	5631.0 ± 67.7c	2209.3 ± 41.2c	83.1 ± 0.1d
Water chestnut	5917.3 ± 51.0d	4337.3 ± 48.0d	1580.0 ± 4.5c	6406.7 ± 43.4d	2069.3 ± 44.4b	63.5 ± 0.0a

Data were means ± standard deviations ($n = 3$). Values in the same column with different letters were significantly different ($p < 0.05$). V_P, peak viscosity; V_H, hot viscosity; V_B, breakdown viscosity; V_F, final viscosity; V_S, setback viscosity; P_{Temp}, pasting temperature.

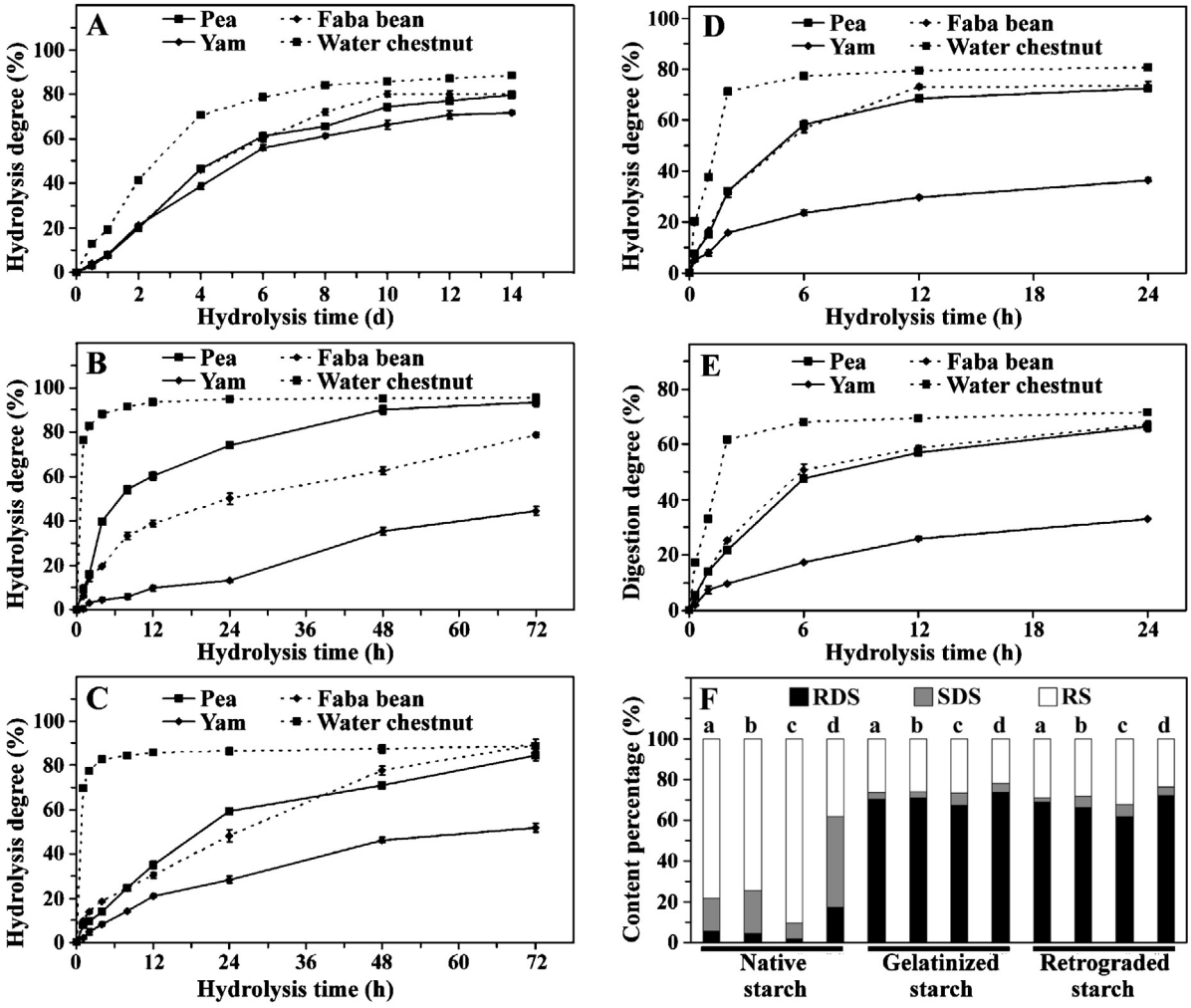

Fig. 5. Hydrolysis and digestion properties of starches. (A–D), the hydrolysis degrees expressed as the percentage of soluble carbohydrates released from native starches by HCl (A), PPA (B), AAG (C) and PPA and AAG (D); (E) the digestion degrees expressed as the percentage of glucose released from native starches by PPA and AAG; (F) the contents of RDS, SDS and RS in native, gelatinized and retrograded starches from pea (a), faba bean (b), yam (c) and water chestnut (d).

PPA and AAG, respectively (Fig. 5B and C). Susceptibility of starch to PPA and AAG attack is influenced by factors such as amylose to amylopectin ratio, crystalline structure, granule size and relative surface area, granule integrity, porosity of granules, and structural inhomogeneities (Blazek & Copeland, 2010). Intact starch granules offer great resistance to enzymatic hydrolysis, the damaged starch is susceptible to enzymatic hydrolysis (de la Hera, Gomez, & Rosell, 2013). The faster enzyme binding is observed for starch with low DSC enthalpy (Warren et al., 2011). The present results showed that water chestnut starch had lower amylose content, lower gelatinization enthalpy, lower ordered structure, higher damaged starch content, and smaller granule size than the other starches. These structural properties led to higher hydrolysis by PPA and AAG.

3.12. Digestion property of starch

In vitro digestion by PPA and AAG is employed to simulate the effects of small intestine hydrolysis and subsequent glycemic response of starch (Englyst et al., 1992). The corms of water chestnut are popularly eaten raw. Therefore, the rate of digestion, which was expressed as the percentage of soluble carbohydrates or glucose released from starch over the time period, was carried out for native starches (Fig. 5D and E). In both situations of soluble carbohydrates and glucose release, water chestnut starch was the most susceptible to digestion, yam starch was the most resistant to digestion, and pea and faba bean starches showed similar digestion degree among four C-type starches. Though the digestion degree of starches by soluble carbohydrate release was similar to that by glucose release, the former was significantly higher than the latter.

For nutritional purposes, starch is classified into three types: RDS, SDS and RS. RDS is rapidly and thoroughly hydrolyzed in the small intestine. SDS is slowly and completely digested in the small intestine, while RS has been considered as the total amount of starch and the products of starch degradation, which resists digestion in the small intestine and functions as a substrate for bacterial fermentation in the large intestine (Englyst et al., 1992). The RDS, SDS and RS contents of pea, faba bean, yam and water chestnut starches were calculated in native, gelatinized and retrograded starches and shown in Fig. 5F. Native starches had extremely lower RDS and higher SDS and RS than gelatinized and retrograded starches. Gelatinized starches had higher RDS and lower RS than retrograded starches. When starch granules in water are exposed to heat, the inter- and intra-molecular hydrogen bonds between starch chains are disrupted, allowing the granules to swell and then disintegrate. The availability of starch chains to the digestive enzymes is thus increased as gelatinization progresses. During gelatinized starch retrogradation, the amylose chains associate to form the amorphous matrix and amylopectins recrystallize to form the crystallites, which increase the resistance to digestive enzymes (Chung, Lim, & Lim, 2006).

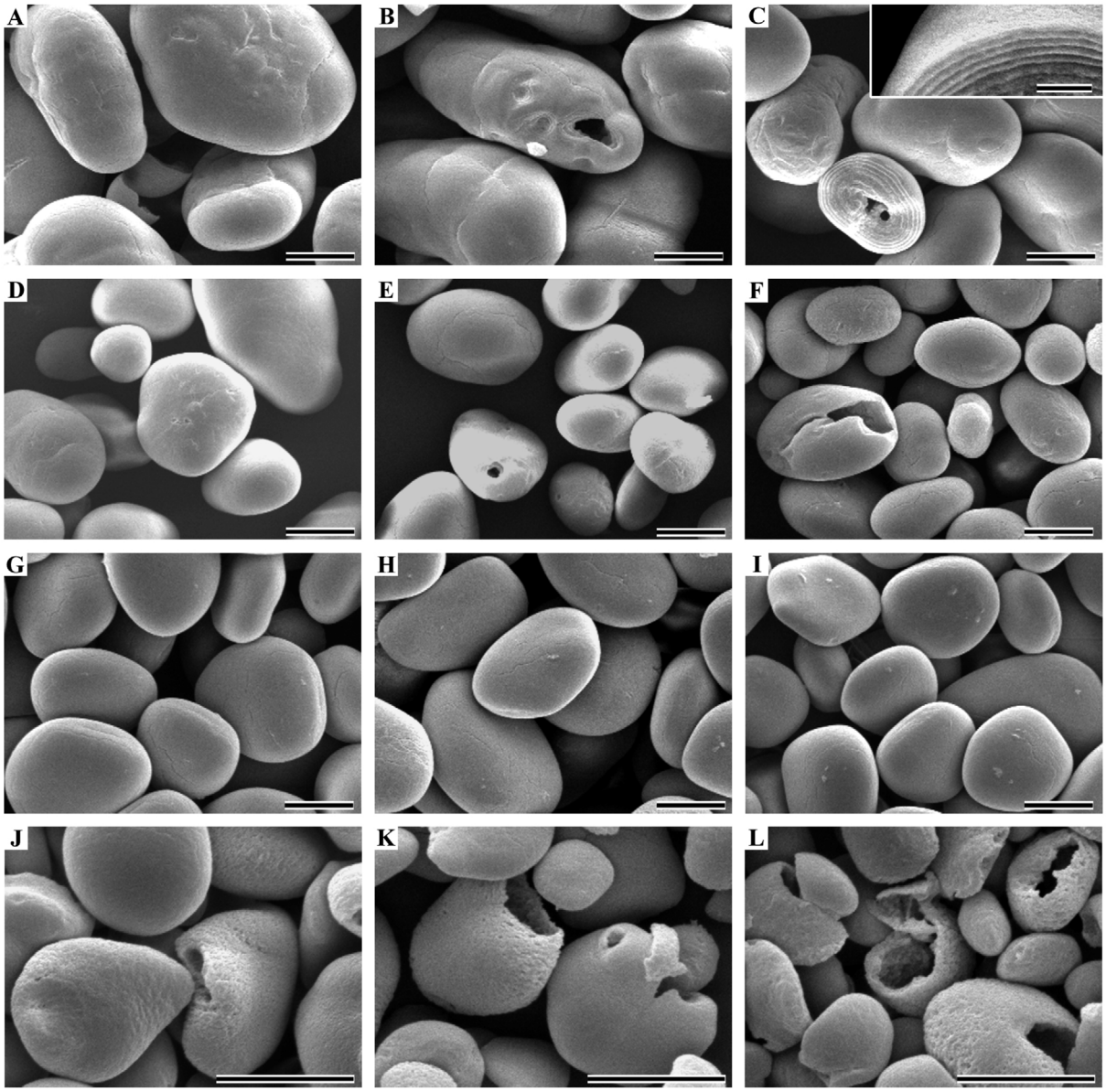

Fig. 6. Scanning electron micrographs of pea (A–C), faba bean (D–F), yam (G–I) and water chestnut (J–L) starch residues digested by PPA and AAG for 20 min (A, D, G, J), 1 h (B, E, H, K) and 2 h (C, F, I, L). Scale bar = 2 μm for the insert of (C) and 10 μm for the others.

In the four C-type starches, water chestnut starch had the highest RDS and lowest RS, yam starch had the lowest RDS and highest RS for native, gelatinized and retrograded starches (Fig. 5F). The differences in the in vitro digestibility among different starches have been attributed to the interplay of many factors such as starch source, granule size, amylose content, branch chain length distribution of amylopectin, degree of crystallinity, polymorphic composition, granular pores, fissures and channels within the granule (Ambigaipalan et al., 2011). The higher enzyme susceptibility of water chestnut starch could be attributed to its smaller granule size, lower amylose content, higher damaged starch content, higher proportion of short amylopectin branch chains, lower gelatinization temperature and enthalpy, higher content of A-type allomorph, and lower ordered degree at granule external region.

The representative SEM micrographs of the residues from native starches digested by PPA and AAG for 20 min, 1 h and 2 h are shown in Fig. 6. For 20 min of digestion, the surface of water chestnut starch granule became rough, and had many pinholes and some grooves and large openings (Fig. 6J). Only sparse pinholes and grooves were observed at the granule surface of pea and faba bean residual starch granules (Fig. 6A and D). Yam residual starch granules did not exhibit significant variations in shape compared with native starch granules (Fig. 6G). For 1 h of digestion, the granule interior was significantly hydrolyzed for water chestnut starch (Fig. 6K), surface erosion and openings were observed for pea and faba bean starch granules (Fig. 6B and E), no significant change was observed for yam starch granule (Fig. 6H). For 2 h of digestion, the empty shell was left for water chestnut starch (Fig. 6L), the interior was degraded for pea and faba bean starch granules (Fig. 6C and F), and yam starch granule did not show significant change at surface (Fig. 6I). The above morphology changes were in agreement with digestion degrees of pea, faba bean, yam and water chestnut starches by PPA and AAG for 20 min, 1 h and 2 h (Fig. 5D and E). After the interiors of starch granules were digested, the granules were easily split open, revealing their internal layered structure as shown in the insert of Fig. 6C. The undigested layered residues were semicrystalline growth rings, which suggested that amorphous growth rings were more susceptible to the digestion by PPA and AAG. PPA and

AAG synergistically hydrolyze native starch via inside-out layer-by-layer degradation pattern. Starch hydrolysis begins with the hydrolytic enzymes access to the interior of the granules via channels and the surface pores. The channels enlarge with concurrent hydrolysis from hilum region toward the outsides. Digestion by enzymes affects the loosely packed internal region of the granules faster than the densely packed periphery, then leaving an empty shell as a result of longer time hydrolysis (Li et al., 2004; Miao, Zhang, Mu, & Jiang, 2011).

4. Conclusion

Native starches were isolated from pea seeds, faba bean seeds, yam rhizomes and water chestnut corms. These starch granules were mostly oval in shape. Pea, faba bean and water chestnut starches had central hila, and yam starch had eccentric hilum. Pea and water chestnut starches had the largest and smallest granule sizes and the highest and lowest amylose contents, respectively. Water chestnut starch had significantly higher damaged starch than the others did. Water chestnut and yam starches had higher amylopectin short and long branch chains, respectively. Yam and pea starches showed typical C-type XRD patterns, and faba bean and water chestnut starches had C_A-type XRD patterns. Water chestnut starch had the highest swelling power, granule swelling and pasting viscosity, lowest gelatinization temperatures and enthalpy among these starches. Faba bean starch had the lowest pasting viscosity, whereas yam starch had the highest pasting and gelatinization temperatures. Water chestnut starch had lower ordered degree in granule external region, and possessed higher hydrolysis degrees of acid, PPA and AAG. Yam starch had higher resistance to hydrolysis of acid, PPA and AAG. Water chestnut starch had higher RDS and lower RS, while yam starch had lower RDS and higher RS. The above structural and functional properties would be useful for the applications of C-type starches in food and nonfood industries.

Acknowledgements

We are very grateful to editor and reviewers for valuable comments, suggestions and corrections. This study was financially supported by grants from the National Natural Science Foundation of China (31071342, 31270221), the New Century Talent Project of Yangzhou University, and the Priority Academic Program Development from Jiangsu Government, China.

References

Ambigaipalan, P., Hoover, R., Donner, E., Liu, Q., Jaiswal, S., Chibbar, R., et al. (2011). Structure of faba bean, black bean and pinto bean starches at different levels of granule organization and their physicochemical properties. *Food Research International*, *44*, 2962–2974.

Atichokudomchai, N., Varavinit, S., & Chinachoti, P. (2004). A study of ordered structure in acid-modified tapioca starch by ^{13}C CP/MAS solid-state NMR. *Carbohydrate Polymers*, *58*, 383–389.

Barrera, G. N., Bustos, M. C., Iturriaga, L., Flores, S. K., León, A. E., & Ribotta, P. D. (2013). Effect of damaged starch on the rheological properties of wheat starch suspensions. *Journal of Food Engineering*, *116*, 233–239.

Blazek, J., & Copeland, L. (2010). Amylolysis of wheat starches. II. degradation patterns of native starch granules with varying functional properties. *Journal of Cereal Science*, *52*, 295–302.

Bogracheva, T. Y., Morris, V. J., Ring, S. G., & Hedley, C. L. (1998). The granular structure of C-type pea starch and its role in gelatinization. *Biopolymers*, *45*, 323–332.

Bogracheva, T. Y., Wang, Y. L., & Hedley, C. L. (2001). The effect of water content on the ordered/disordered structures in starches. *Biopolymers*, *58*, 247–259.

Borén, M., Glaring, M. A., Ghebremedhin, H., Olsson, H., Blennow, A., & Jansson, C. (2008). Molecular and physicochemical characterization of the high-amylose barley mutant Amo1. *Journal of Cereal Science*, *47*, 79–89.

Buléon, A., Gérard, C., Riekel, C., Vuong, R., & Chanzy, H. (1998). Details of the crystalline ultrastructure of C-starch granules revealed by synchrotron microfocus mapping. *Macromolecules*, *31*, 6605–6610.

Butardo, V. M., Daygon, V. D., Colgrave, M. L., Campbell, P., Resurreccion,. M., Cuevas, A., et al. (2012). Biomolecular analyses of starch and starch granule proteins in the high-amylose rice mutant Goami 2. *Journal of Agricultural and Food Chemistry*, *60*, 11576–11585.

Cai, C. H., & Wei, C. X. (2013). In situ observation of crystallinity disruption patterns during starch gelatinization. *Carbohydrate Polymers*, *92*, 469–478.

Cai, L. M., & Shi, Y. C. (2010). Structure and digestibility of crystalline short-chain amylose from debranched waxy wheat, waxy maize, and waxy potato starches. *Carbohydrate Polymers*, *79*, 1117–1123.

Carciofi, M., Blennow, A., Jensen, S. L., Shaik, S. S., Henriksen, A., Buléon, A., et al. (2012). Concerted suppression of all starch branching enzyme genes in barley produces amylose-only starch granules. *BMC Plant Biology*, *12*, 223.

Cheetham, N. W. H., & Tao, L. (1998). Variation in crystalline type with amylose content in maize starch granules: an X-ray powder diffraction study. *Carbohydrate Polymers*, *36*, 277–284.

Chung, H. J., Lim, H. S., & Lim, S. T. (2006). Effect of partial gelatinization and retrogradation on the enzymatic digestion of waxy rice starch. *Journal of Cereal Science*, *43*, 353–359.

Chung, H. J., & Liu, Q. (2012). Physicochemical properties and *in vitro* digestibility of flour and starch from pea (*Pisum sativum* L.) cultivars. *International Journal of Biological Macromolecules*, *50*, 131–137.

Crépon, K., Marget, P., Peyronnet, C., Carrouée, B., Arese, P., & Duc, G. (2010). Nutritional value of faba bean (*Vicia faba* L.) seeds for feed and food. *Field Crops Research*, *115*, 329–339.

de la Hera, E., Gomez, M., & Rosell, C. M. (2013). Particle size distribution of rice flour affecting the starch enzymatic hydrolysis and hydration properties. *Carbohydrate Polymers*, *98*, 421–427.

Englyst, H. N., Kingman, S. M., & Cummings, J. H. (1992). Classification and measurement of nutritionally important starch fractions. *European Journal of Clinical Nutrition*, *45*, S33–S50.

Harrigan, K. A. (1997). Particle size analysis using automated image analysis. *Cereal Foods World*, *42*, 30–35.

Hizukuri, S. (1985). Relationship between the distribution of the chain length of amylopectin and the crystalline structure of starch granules. *Carbohydrate Research*, *141*, 295–306.

Hodge, W. H. (1956). Chinese water chestnut or matai—A paddy crop of China. *Economic Botany*, *10*(1), 49–65.

Konik-Rose, C., Thistleton, J., Chanvrier, H., Tan, I., Halley, P., Gidley, M., et al. (2007). Effects of starch synthase IIa gene dosage on grain, protein and starch in endosperm of wheat. *Theoretical and Applied Genetics*, *115*, 1053–1065.

Li, J. H., Vasanthan, T., Hoover, R., & Rossnagel, B. G. (2004). Starch from hull-less barley: V. In-vitro susceptibility of waxy, normal, and high-amylose starches towards hydrolysis by alpha-amylases and amyloglucosidase. *Food Chemistry*, *84*, 621–632.

Man, J. M., Cai, J. W., Cai, C. H., Xu, B., Huai, H. Y., & Wei, C. X. (2012). Comparison of physicochemical properties of starches from seed and rhizome of lotus. *Carbohydrate Polymers*, *88*, 676–683.

Miao, M., Zhang, T., Mu, W., & Jiang, B. (2011). Structural characterizations of waxy maize starch residue following *in vitro* pancreatin and amyloglucosidase synergistic hydrolysis. *Food Hydrocolloids*, *25*, 214–220.

Morrison, W. R., Tester, R. F., & Gidley, M. J. (1994). Properties of damaged starch granules. II. Crystallinity, molecular order and gelatinisation of ball-milled starches. *Journal of Cereal Science*, *19*, 209–217.

Morton, J. F. (1988). Chinese water chestnuts in Florida—Past, present, and future. *Proceedings of the Florida State Horticultural Society*, *101*, 139–144.

Noda, T., Tsuda, S., Mori, M., Takigawa, S., Matsuura-Endo, C., Saito, K., et al. (2004). The effect of harvest dates on the starch properties of various potato cultivars. *Food Chemistry*, *86*, 119–125.

Sandhu, K. S., Singh, N., & Kaur, M. (2004). Characteristics of the different corn types and their grain fractions: physicochemical, thermal, morphological, and rheological properties of starches. *Journal of Food Engineering*, *64*, 119–127.

Sasaki, T., & Matsuki, J. (1998). Effect of wheat starch structure on swelling power. *Cereal Chemistry*, *75*, 525–529.

Sevenou, O., Hill, S. E., Farhat, I. A., & Mitchell, J. R. (2002). Organisation of the external region of the starch granule as determined by infrared spectroscopy. *International Journal of Biological Macromolecules*, *31*, 79–85.

Shi, Y. C., Capitani, T., Trzasko, P., & Jeffcoat, R. (1998). Molecular structure of a low-amylopectin starch and other high-amylose maize starches. *Journal of Cereal Science*, *27*, 289–299.

Simsek, S., Tulbek, M. C., Yao, Y., & Schatz, B. (2009). Starch characteristics of dry peas (*Pisum sativum* L.) grown in the USA. *Food Chemistry*, *115*, 832–838.

Singh, N., Kaur, L., Ezekiel, R., & Guraya, H. S. (2005). Microstructural, cooking and textural characteristics of potato (*Solanum tuberosum* L.) tubers in relation to physicochemical and functional properties of their flours. *Journal of the Science of Food and Agriculture*, *85*, 1275–1284.

Song, Y., & Jane, J. (2000). Characterization of barley starches of waxy, normal, and high amylose varieties. *Carbohydrate Polymers*, *41*, 365–377.

Tester, R. F. (1997). Properties of damaged starch granules: composition and swelling properties of maize, rice, pea and potato starch fractions in water at various temperatures. *Food Hydrocolloids*, *11*, 293–301.

Tester, R. F., & Karkalas, J. (1996). Swelling and gelatinization of oat starches. *Cereal Chemistry*, *73*, 271–273.

Viles, F. J., & Silverman, L. (1949). Determination of starch and cellulose with anthrone. *Analytical Chemistry*, *21*, 950–953.

Wang, L., Yin, Z. H., Zhang, Y., Xie, B. J., & Sun, Z. D. (2008). Morphological, physicochemical and textural properties of starch separated from Chinese water chestnut. *Starch*, *60*, 181–191.

Wang, S. J., Liu, H. Y., Gao, W. Y., Chen, H. X., Yu, J. G., & Xiao, P. G. (2006). Characterization of new starches separated from different Chinese yam (*Dioscorea opposita* Thunb.) cultivars. *Food Chemistry*, *99*, 30–37.

Wang, S. J., Yu, J. L., Zhu, Q. H., Yu, J. G., & Jin, F. M. (2009). Granular structure and allomorph position in C-type Chinese yam starch granule revealed by SEM, ^{13}C CP/MAS NMR and XRD. *Food Hydrocolloids*, *23*, 426–433.

Wang, Y. J., White, P., Pollak, L., & Jane, J. (1993). Characterization of starch structures of 17 maize endosperm mutant genotypes with Oh43 inbred line background. *Cereal Chemistry*, *70*, 171–179.

Warren, F. J., Royall, P. G., Gaisford, S., Butterworth, P. J., & Ellis, P. R. (2011). Binding interactions of α-amylase with starch granules: The influence of supramolecular structure and surface area. *Carbohydrate Polymers*, *86*, 1038–1047.

Wei, C. X., Qin, F. L., Zhou, W. D., Xu, B., Chen, C., Chen, Y. F., et al. (2011). Comparison of the crystalline properties and structural changes of starches from high-amylose transgenic rice and its wild type during heating. *Food Chemistry*, *128*, 645–652.

Wei, C. X., Qin, F. L., Zhu, L. J., Zhou, W. D., Chen, Y. F., Wang, Y. P., et al. (2010). Microstructure and ultrastructure of high-amylose rice resistant starch granules modified by antisense RNA inhibition of starch branching enzyme. *Journal of Agricultural and Food Chemistry*, *58*, 1224–1232.

Wei, C. X., Xu, B., Qin, F. L., Yu, H. G., Chen, C., Meng, X. L., et al. (2010). C-type starch from high-amylose rice resistant starch granules modified by antisense RNA inhibition of starch branching enzyme. *Journal of Agricultural and Food Chemistry*, *58*, 7383–7388.

Xu, S. Y., & Shoemaker, C. F. (1986). Gelatinization properties of Chinese water chestnut starch and lotus root starch. *Journal of Food Science*, *51*, 445–449.